Expanding TRANS4D's Scope to Include 3-D Crustal Velocity Estimates for a Neighborhood of the Caribbean Plate

Richard Snay[1], Jarir Saleh[2], Michael Dennis[2], Charles DeMets[3], and Héctor Mora-Páez[4]

1. Corresponding author, retired, formerly of the National Geodetic Survey, 427 Homewood Circle, Frederick, Maryland, 21702, USA. Email: rssnay@aol.com
2. National Geodetic Survey, Silver Spring, Maryland, USA
3. Department of Geoscience, University of Wisconsin, Madison, Wisconsin, USA
4. Space Geodesy Research Group, Geological Survey of Colombia, Bogota 111321, Colombia

Abstract

This paper introduces version 0.3 of the TRANS4D software, where TRANS4D is short for "Transformations in Four Dimensions". TRANS4D enables geospatial professionals and others to transform 3-D positional coordinates across time and among several popular terrestrial reference frames. Version 0.3 includes a crustal velocity model for a neighborhood of the Caribbean plate in the form of 3-D crustal velocity estimates at the nodes of a 2-D grid in latitude and longitude. This velocity model supplements existing TRANS4D velocity models for the continental U.S. and for parts of Alaska and Canada. This paper also introduces a terrestrial reference frame, called CATRF2014, which was derived from horizontal crustal velocities for 25 geodetic stations. These stations are considered to be located within the "stable" interior of the Caribbean plate because each has a horizontal velocity whose magnitude is less than 1.0 mm/yr relative to CATRF2014. This new reference frame is defined in terms of a 3-parameter transformation from the International GNSS Service 2014 (IGS14) reference frame, which can be considered identical to the International Terrestrial Reference Frame of 2014 (ITRF2014). These parameters estimate the Euler-pole parameters that characterize the motion of the "stable" interior of the Caribbean plate relative to IGS14.

Introduction

Snay et al. (2016) introduced numerical models that quantify three-dimensional (3-D) crustal velocities as a function of latitude and longitude for the conterminous United States (CONUS) and for most of Alaska and Canada. These models provide the foundation for version 0.1 of the TRANS4D software, where TRANS4D is short for "Transformations in Four Dimensions". TRANS4D is being developed to enable geospatial professionals and others to apply estimated velocities when transforming 3-D positional coordinates referred to one date to corresponding

3-D positional coordinates referred to an alternative date. Moreover, users can apply TRANS4D to transform positional coordinates from one terrestrial reference frame to another for a suite of popular reference frames, including all existing realizations of the International Terrestrial Reference System, plus all existing reference frames of the International GNSS Service (IGS) and the World Geodetic System 1984, as well as three regional frames of the North American Datum of 1983 (referenced to the North America, Pacific, and Mariana tectonic plates, respectively). TRANS4D also addresses changes in positional coordinates due to phenomena other than constant velocities. In particular, TRANS4D contains models quantifying the coseismic displacements associated with 31 North American earthquakes and a model for the postseismic motion associated with the M7.9 Denali Fault earthquake that occurred in central Alaska on 3 November 2002. This document, however, will address only that crustal motion associated with constant velocities.

TRANS4D's velocity models include a collection of 2-D grids (in latitude and longitude) where each grid spans a specified spherical rectangle and where an estimated 3-D velocity (north-east-up components) is recorded for each grid node, together with the three standard deviations associated with these three velocity components. For each point located within the span of a given rectangular grid, TRANS4D employs bilinear interpolation to estimate the point's 3-D velocity and its associated three standard deviations from the corresponding values stored at the four nodes that define the grid cell encompassing the location of interest.

The velocity models encoded in TRANS4D have been derived from repeated geodetic observations−primarily GNSS observations−but leveling, trilateration, and other geodetic data types have also been employed. Thanks to the rapid increase in the number of continuously operating GNSS stations distributed around the world, velocity models

can be upgraded relatively frequently. Accordingly, version 0.2 of TRANS4D was recently released [Snay et al., 2018]. Version 0.2 provides a much-improved velocity model for that part of CONUS located west of longitude 107°W. The more accurate velocities residing in version 0.2 benefitted from the use of an improved velocity-interpolation algorithm compared to that used for the original TRANS4D version, as well as longer observational histories at many of the sites involved in version 0.1. Also, version 0.2 benefitted from the existence of estimated velocities at many additional geodetic stations.

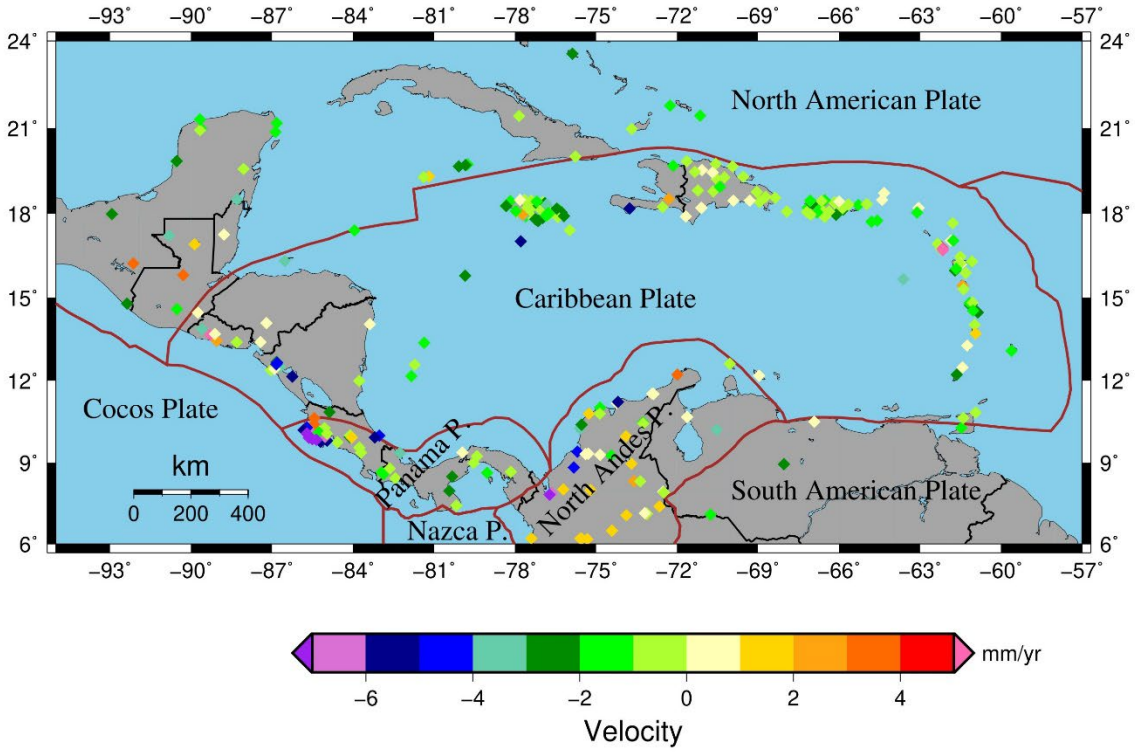

Fig. 1. The Caribbean study area. Colored diamonds identify geodetic stations at which IGS14 vertical velocities have been estimated with standard deviations $\leq$ 2.0 mm/yr. Each diamond's color reflects the station's stage-2 IGS14 vertical velocity (see text for definition of "stage-2"). Brown line segments approximate tectonic plate boundaries. Black line segments denote national borders.

In this document, version 0.3 of TRANS4D is introduced. This new version includes a 3-D velocity model for a spherical rectangle encompassing a neighborhood of the Caribbean plate. This rectangle ranges between latitudes 6°N and 24°N and between longitudes 57°W and 95°W. Its associated velocity grid has a mesh of 0.0625°-by-0.0625°. Figure 1 displays the area spanned by this grid together with geodetic stations involved in estimating a 3-D velocity at each node of this grid. Moreover, Figure 1 identifies seven tectonic plates and/or microplates that collectively span this spherical rectangle. The plate boundaries presented in Figure 1 reflect those provided by the digital model published by Bird (2003).

This document also introduces estimates for the three parameters that quantify the Euler Pole and the rotation rate about this pole, which may be applied to define a transformation from the IGS14 reference frame (Rebischung and Schmidt, 2016) to a new terrestrial reference frame in which the transformed horizontal velocities of 25 existing geodetic stations each has a magnitude less than 1.0 mm/yr. Hence, these 25 stations are thought to be located within the "stable" interior of the Caribbean plate. This new terrestrial reference frame is herein referred to as CATRF2014,

as it constitutes a preliminary realization of the Caribbean Terrestrial Reference Frame of 2022 (CATRF2022) to be developed by the National Geodetic Survey (NGS) − an office of the National Oceanic and Atmospheric Administration (NOAA) − in the 2024-2025 timeframe (NGS, 2020). (Note that NGS does not recognize CATRF2014 as an official reference frame for general use. CATRF2014 was developed only for research and instructional purposes.)

Because the CATRF2014 realization was derived using GNSS data referred to IGS14, it is formally defined with respect to the IGS14 reference frame. IGS14 is a GNSS-only solution aligned with the International Terrestrial Reference Frame of 2014 (ITRF2014) at epoch 2010.00 (Altamimi et al., 2016; Rebischung et al., 2016). Therefore, IGS14 can be considered equivalent to ITRF2014 from a frame definition and transformation perspective (and they are treated as identical within TRANS4D).

Throughout this paper, the vertical velocity at a point refers to the rate of change over time of the ellipsoidal height at this point relative to an ellipsoid whose size and shape equal those adopted for the Geodetic Reference System of 1980 (Moritz, 2000).

Geodetic Data

The new 3-D velocity model for the Caribbean has been formulated by using velocity vectors derived from geodetic observations. These velocity vectors were obtained from 16 separate data sets provided by multiple institutions and researchers. In many cases, a velocity vector contained in one data set may have been computed from essentially the same geodetic data used to compute a velocity vector contained in another data set. The 16 data sets include the following:

- The IGS data set based on continuous GNSS data observed between 2 January 1994 and 30 December 2018 at more than 1,500 IGS-affiliated stations distributed around the world (ftp://cddis.gsfc.nasa,gov/gps/products/2033/IGS18P52_all.ssc.Z). The IGS updates its solution on a weekly basis. These velocities are referred to the IGS14 reference frame.
- A data set published by Wang et al. (2019) consisting of 3-D velocity vectors derived from GPS data observed between 2012 and 2018 at 250 continuously operating GNSS stations located on or near the Caribbean plate. These velocities are referred to the CARIB18 reference frame whose development is described in that publication.
- A data set published by Ellis et al. (2018) consisting of IGS08-consistent 2-D horizontal velocities derived from GPS data observed (some continuously others in campaign mode) between 1999 and 2017 at 201 geodetic stations located in northern Central America and southern Mexico. Ellis et al. (2019) discuss the implications of these velocities in great detail.
- An unpublished set of IGS14 consistent 3-D velocities provided by Charles DeMets and derived from GNSS data observed between 1998 and 2020 at 50 stations located in the vicinity of Jamaica.
- The 2017 SIRGAS (Sistema de Referencia Geocéntrico para las Americas) solution which provides IGS14-consistent 3-D velocities for continuously operating GNSS stations distributed throughout parts of South America and North America. These velocities are based on GNSS data observed between 2011 and 2017, and they are available at https://doi.pangaea.de/10.1594/PANGAEA.912349. Sánchez and Drewes (2020) discuss the implications of these velocities in great detail.
- A data set published by Mora-Páez et al. (2019) containing ITRF2008-consistent 2-D horizontal velocity vectors derived from GPS data (observed prior to 2016) at 60 continuously operating stations located in northwestern South America and the southwest Caribbean.
- An unpublished set of ITRF2014-consistent 3-D velocities for 69 continuously observed GNSS stations located throughout this paper's study area, but with a concentration located in the vicinity of Colombia. These velocities were computed by the Space Geodesy Research Group of the Geohazards Directorate, Geological Survey of Colombia.
- A data set produced by Saleh et al. (2021) which provides IGS14-consistent 3-D velocity vectors derived from GPS data observed between 1996 and 2017 at approximately 2,393 geodetic stations including those in NOAA's Continuously Operating Reference Station (CORS) network plus many contained in the IGS-affiliated network. The adopted CORS velocities may be obtained at ftp://cors.ngs.noaa.gov/cors/coord/coord_14/itrf2014_geo.comp.txt .

- A data set produced by NASA's Jet Propulsion Laboratory which provides IGS14-consistent 3-D velocities for more than 2,650 continuous GNSS stations distributed around the world. The latest results are available at https://sideshow.jpl.nasa.gov/post/tables/table2.html .
- An unpublished data set produced in 2019 by Natural Resources Canada (NRCan) for 3-D velocities (some observed continuously others in campaign mode) at geodetic stations located in and around Canada (Michael Craymer, personal communication, 2019).

Three of the remaining six data sets are updated versions of the data sets used by Snay et al. (2018). They include:

- A data set produced by the University of Nevada Reno (UNR) (Blewitt et al., 2018) which provides estimated IGS14-consistent 3-D velocities for more than 10,400 continuous GNSS stations distributed around the world. The latest UNR velocities are available at http://geodesy.unr.edu.
- A data set produced by GAGE (Geodesy Advancing Geosciences and Earthscope) which includes IGS14-consistent 3-D velocities for more than 2,600 continuous GNSS stations distributed around the world, including those contained in UNAVCO's Plate Boundary Observatory (PBO) (Herring et al., 2016). The GAGE velocities are updated annually with the latest results available at ftp://data-out.unavco.org/pub/products /velocity/cwu.snaps_igs14.vel .
- A MEaSUREs (Making Earth System data records for Use in Research Environments) data set that NASA's Jet Propulsion Laboratory and Scripp's Orbit and Permanent Array Center jointly produce (Bock and Webb, 2012). This data set provides IGS08-consistent 3-D velocities for more than 2,600 continuous GNSS stations distributed around the world. The MEaSUREs velocities are updated weekly with the latest results being available at http://geoapp03.ucsd.edu/gridshere/gridsphere .

The three remaining data sets are the same as those used by Snay et al. (2016, 2018). They include:

- A data set published by McCaffrey et al. (2013) for GPS stations (some observed continuously others in campaign mode) located in and around northwestern CONUS.
- The Southern California Earthquake Center data set known as "Crustal Motion Model Four" (Shen et al., 2011) for geodetic stations located mainly in and around southern California.
- An unpublished data set produced by the University of Alaska Fairbanks for 3-D velocities at geodetic stations (some observed continuously others in campaign mode) located in and around Alaska (Jeffrey Freymueller, personal communication, 2014).

While these latter three data sets do not contribute directly to determining IGS14-consistent 3-D velocities at geodetic stations located in and around the Caribbean plate, these data sets have been included to help transform the velocities of the 16 data sets from their adopted reference frames into the IGS14 reference frame, as discussed in the following paragraph.

Using the combination process described in Appendix A of Snay et al. (2016), the GNSS derived velocities from these 16 data sets were employed to estimate a single 3-D IGS14 velocity for each of approximately 13,700 distinct geodetic stations. Of these stations, approximately 529 reside either within the chosen spherical rectangle for this paper or within approximately 100 km of this spherical rectangle. The remaining stations span the globe. Velocities at stations located around the world were included in the combination process to more accurately estimate the seven parameters required for each of the 16 data sets to transform its velocities from its associated reference frame to the IGS14 reference frame. Actually, a set of seven parameters is needed for each of only 15 of the data sets because the velocities of the IGS data set are already referred to IGS14. The seven parameters include three translation rates ($\dot{T}_X$, $\dot{T}_Y$, $\dot{T}_Z$), three rotation rates ($\dot{R}_X$, $\dot{R}_Y$, $\dot{R}_Z$), and a scale change rate ($\dot{S}$). Here the subscripts – *X, Y, Z* – pertain to the three axes of a traditional right-handed Earth-centered-Earth-fixed (ECEF) Cartesian coordinate system with the *Z*-axis approximating Earth's axis of rotation and the positive *X*-axis piercing Earth's equator near 0° longitude. See Snay et al. (2016) for additional information about the employed combination process.

In this publication, velocities contained in the 16 data sets are referred to as "stage-1" velocities; and the velocities estimates produced via the combination process are referred to as "stage-2" velocities. The diamonds appearing in Figure 1 identify GNSS stations located in the spherical rectangle of this study. The color of each diamond corresponds to the station's stage-2 vertical velocity. In subsequent sections of this document, a two-step process is discussed which employs the stage-2 velocities to estimate IGS14 velocities at the grid nodes of the specified spherical rectangle. The resulting velocities at these nodes are referred to as "stage-3" velocities. Stage-3 velocities correspond to the velocities encoded into the TRANS4D software.

The standard deviation assigned to a stage-2 velocity component (east-north-up) of a geodetic station equals the minimum value of the reported standard deviations, pertaining to this velocity component, among all of the stage-1 velocities at this station with the following restrictions: (1) the standard deviation of a stage-2 horizontal velocity component cannot be smaller than 0.2 mm/yr and (2) the standard deviation of a stage-2 vertical velocity component cannot be smaller than 0.3 mm/yr. These lower bounds are consistent with the results presented in Figure 2 of Saleh et al. (2021). The standard deviation of a stage-2 velocity component was assigned in this way because the various stage-1 velocities for a station are based upon very similar sets of geodetic data and thus do not represent independent estimates. Also, it is not uncommon for different institutions to estimate different velocities with different standard deviations at a station even though they are using essentially the same data for that station.

Modeling Velocities

The employed velocity-modeling process is a two-step procedure that uses stage-2 velocities to estimate stage-3 velocities. Snay et al. (2018) discuss this process in some detail, thus only an outline is presented here. For the first step (called Step A), a preliminary model for the 3-D velocity field is specified. This preliminary model may be imported from a previous study. Alternatively, this preliminary model may be developed by using equations to characterize velocities in terms of relevant parameters. For the second step (called Step B), a residual velocity is calculated for each available stage-2 velocity located in the designated study area by subtracting from each stage-2 velocity its corresponding velocity yielded by the preliminary model. Then the interpolation process, discussed in the following paragraph, is applied to the set of residual velocities to estimate an incremental velocity for each of several designated points located in the study area. For this study, these designated points will be the nodes of a 2-dimensional grid spanning the previously specified spherical rectangle. Each of these incremental velocities are then added to its corresponding velocity, as generated via the preliminary model, to produce a stage-3 velocity. Thus, via bilinear interpolation, the resulting set of stage-3 velocities at the specified collection of grid nodes forms the foundation for an updated velocity model for all points located within the designated spherical rectangle.

In this document, the spatial interpolation of the residual velocities is performed one component at a time (north, east, up) using all available residual velocities located within a “prespecified distance” of the location at which an estimated (residual) velocity is desired. The applied interpolation process is a variation of kriging (Goovaerts, 1997). In particular, for each component of the residual velocities, a function needs to be estimated which relates the semivariance between two available residual velocities to the distance between their respective locations. For each (residual) velocity component at a specified location, this function dictates how much each of the available residual velocities contributes to the estimated value of that component. For mathematical details, see Snay et al. (2018).

For this study, a “prespecified distance” of 100 km was used except when the resulting circular area around a given location contained less than 7 residual velocities, in which case the “prespecified distance” was increased to 200 km. This exception was sometimes required to estimate residual velocities on isolated islands or at oceanic points located far from major land masses.

For this study, the employed preliminary model was such that IGS14 vertical velocities are equal to 0.0 mm/yr at all location and the IGS14 horizontal velocities are equal to those defined by a rigid plate motion model for each of the seven tectonic plates/microplates residing, in whole or part, within the Caribbean study area as pictured in Figure 1. This adopted set of plate motion models is discussed later in this paper. For now, however, it is somewhat apparent that the estimated 3-D velocity may be relatively crude because, for example, the tectonic plates are initially assumed to be fully rigid (and thus have essentially no vertical velocity), whereas each plate usually undergo significant horizontal and vertical deformation near its boundaries with other plates. Thus, the process may need to be iterated. That is, the resulting stage-3 estimates for the 3-D velocities may need to serve as the preliminary velocities for a second solution in which the newer residual velocity should be smaller in magnitude than the original residual velocities. For this study, the estimation process was performed four times, with each successive solution relying on the results of its immediately previous solution.

Estimated Vertical Velocities

Figure 2 presents a map of the resulting stage-3 IGS14 vertical velocities found (after the fourth solution) within the larger land masses located in the adopted study area. Note that such velocities are not shown at places located more than 200 km from any geodetic station included in this study, and they are also not shown outside any land masses (even though TRANS4D may provide such velocity estimates via interpolation). Also, velocities are not shown at places where the standard deviations for these estimated velocities exceed 2.0 mm/yr. The TRANS4D software,

however, will output an IGS14 vertical velocity of 0.0 mm/yr for those points located more than 200 km from any geodetic station used in this study, and this software will assign a nominal value of 2.2 mm/yr for the standard deviation of this velocity. Note that TRANS4D may yield a nonzero vertical velocity when it transforms a zero-value IGS14 vertical velocity from IGS14 to its corresponding vertical velocity relative to a different reference frame (an inevitable consequence of frame transformations). Figure 3 presents a map displaying standard deviations for the stage-3 IGS14 vertical velocities located within the larger land masses.

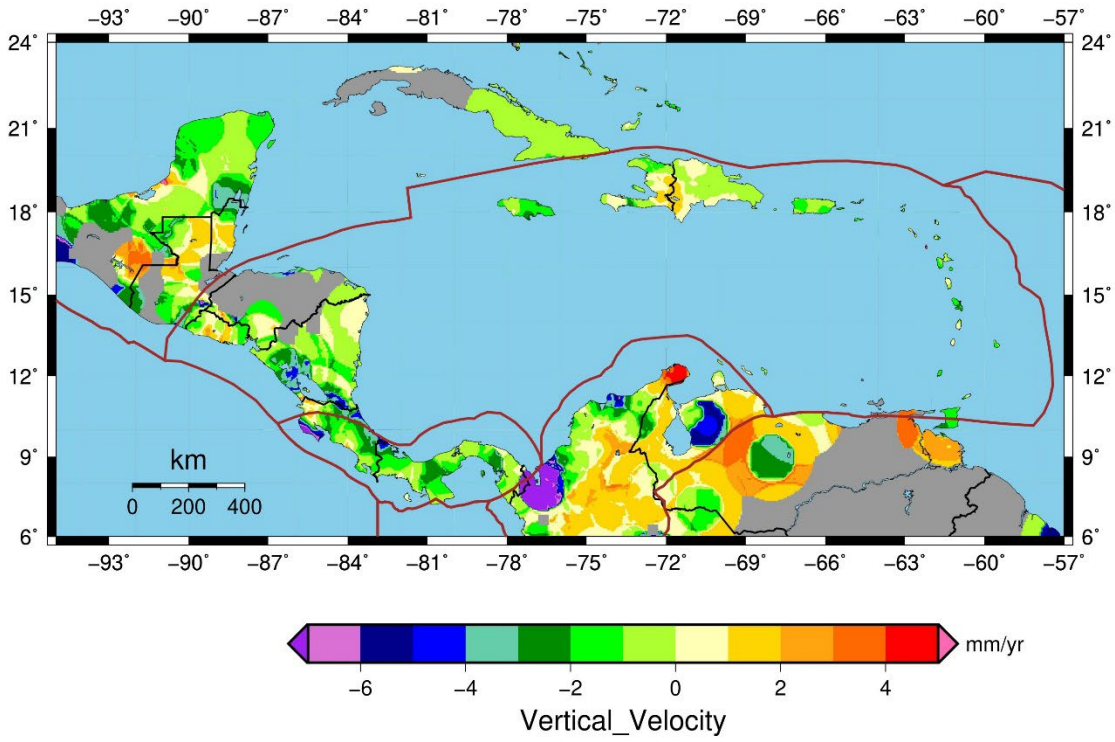

Fig. 2. Map of stage-3 IGS14 vertical velocities at locations within the larger land masses. Gray areas identify locations where the standard deviations for these vertical velocities exceed 2.0 mm/yr.

Estimating Euler-Pole parameters

Figure 4 presents the collection of stage-2 horizontal velocities relative to a horizontal reference frame defined by a newly determined Euler pole for the Caribbean plate. This Euler-pole reference frame minimizes horizontal velocities at selected locations on the Caribbean plate so as to emphasize where this plate is relatively stable and how other locations are moving relative to these "stable" locations. As such, the display of the horizontal velocity field relative to this Euler-pole-defined reference frame is more instructive than a display of the IGS14 horizontal velocity field.

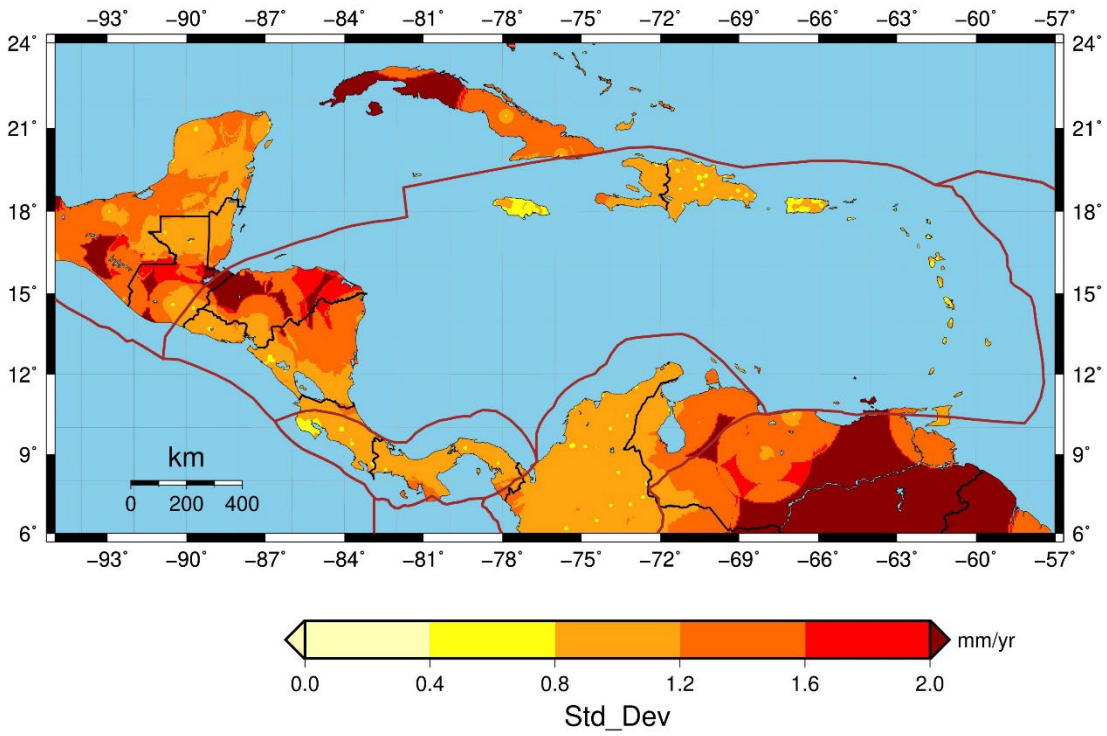

Fig. 3. Map of standard deviations for stage-3 IGS14 vertical velocities at locations within the larger land masses.

The designation of the Euler-pole parameters involves the determination of three parameters relative to some adopted reference frame. For this study, IGS14 serves as the adopted reference frame. Moreover, two of the three parameters correspond to the latitude φ and longitude λ at which a pole (that passes through the geocenter) pierces the Earth's surface and the third parameter is a rotation rate ω of the Earth's surface relative to this pole. Alternatively, the Euler pole can be quantified by designating three rotation rates, namely, a rotation rate about the X-axis (ω_X), another about the Y-axis (ω_Y), and another about the Z-axis (ω_Z) where (X, Y, Z) represent the three axes of an ECEF coordinate system with the X- and Y-axes located in the plane of the equator and with the Z-axis approximating Earth's axis of rotation. The two Euler pole representations are related by the three equations:

$$\omega_X = \omega \cdot \cos\varphi \cdot \cos\lambda \qquad (1)$$

$$\omega_Y = \omega \cdot \cos\varphi \cdot \sin\lambda$$

$$\omega_Z = \omega \cdot \sin\varphi$$

To obtain values for the three rotation rates $(\omega_X, \omega_Y, \omega_Z)$, the stage-2 IGS14 horizontal velocities of the available 303 geodetic stations (that reside on the Caribbean plate), were employed in a weighted least squares estimation process. This process yielded estimates for the three rotation rates which minimize the horizontal velocities that resulted by applying the estimated rotation rates to the weighted IGS14 velocities of the involved stations. (Note that the weight assigned to a stage-2 horizontal velocity component was set to $1.0/\sigma^2$ where σ represents the estimated standard deviation of this velocity component.)

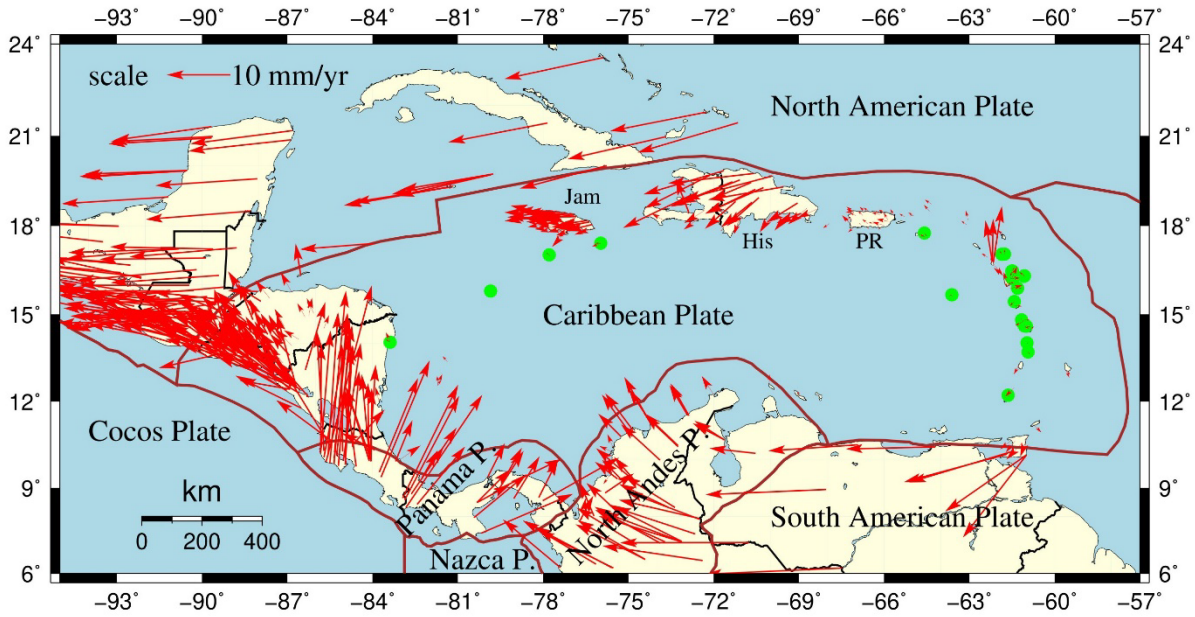

Fig. 4. Stage-2 horizontal velocities relative to a reference frame in which the "stable" part of the Caribbean plate is held fixed. The green disks identify the 25 geodetic stations employed to estimate the Euler-pole parameters defining this reference frame. Jam = Jamaica, His = Hispaniola, and PR = Puerto Rico.

More specifically, if (*Xa, Ya, Za*) represent the IGS14 coordinates of a point, located on the Caribbean plate, whose estimated IGS14 velocity equals (V_{Xa}, V_{Ya}, V_{Za}), and if a rotation rate (ω_X, ω_Y, ω_Z) were applied to the IGS14 coordinates to produce a new reference frame, then the resulting velocities (V_{Xb}, V_{Yb}, V_{Zb}), that are relative to this new frame, would be adequately approximated by the equations:

$$V_{Xb} = V_{Xa} + (\omega_Z)\cdot Ya - (\omega_Y)\cdot Za \qquad (2)$$

$$V_{Yb} = V_{Ya} - (\omega_Z)\cdot Xa + (\omega_X)\cdot Za$$

$$V_{Zb} = V_{Za} + (\omega_Y)\cdot Xa - (\omega_X)\cdot Ya$$

when ω_X, ω_Y, and ω_Z are each small in magnitude.

Thus, using least squares estimation, one can estimate the values of ω_X, ω_Y, and ω_Z that best minimize the velocities (V_{Xb}, V_{Yb}, V_{Zb}) for some subset of geodetic stations residing on the Caribbean plate. As may be expected, when all 303 stations, residing on this plate, were involved, the resulting horizontal velocities at some of these stations were relatively large, especially those stations located near the periphery or unstable part of the Caribbean plate. Hence, certain geodetic stations, having the larger resulting horizontal velocities, were eliminated before performing a subsequent application of the estimation process to the remaining stations. This elimination procedure was iterated until all of the remaining stations had rotated horizontal velocities each of whose magnitude is smaller than 1.0 mm/yr. Despite having such low velocities, several of the remaining stations reside within or near deforming tectonic blocks located within the Caribbean plate. These deforming blocks are identified in Figure 8 of Symithe et al. (2015). Moreover, these blocks are located in the vicinity of Jamaica, Hispaniola, and/or Puerto Rico (see Figure 4 to locate these three islands) or within 100 km of the South American coastline. Thus, for the sake of caution, the geodetic stations residing on or near these deforming blocks were excluded when further estimating the Caribbean

Euler-pole parameters relative to IGS14. In the end, only 25 of the 303 stations, residing on the Caribbean plate, were effectively involved in determining the desired Euler-pole parameters. These 25 stations are listed in Table 1, and they are displayed as green disks in Figures 4 and 5. Note that all but four of these 25 stations reside in the eastern sector of the Caribbean plate. This distribution reflects a sampling problem in that the geodetic coverage of the Caribbean plate is poorly distributed because most of this plate resides under water. In addition, most of the 303 stations are located near the edge of the plate, where significant deformation occurs. The values of the three estimated rotation rates are

$$(\omega_X, \omega_Y, \omega_Z) = (-0.188, -4.730, 2.963) \text{ nrad/yr} \quad (3)$$

whose respective standard deviations have the estimated values of (0.032, 0.066, 0.022) nrad/yr. Note that nrad is short for nanoradian, that is, 10^{-9} radians.

Table 1. Horizontal stage-2 velocities at the 25 geodetic stations used to estimate Euler-pole parameters for the Caribbean plate

Site	Latitude	Longitude	IGS14 velocity ± std. dev.		Velocity relative to stable Caribbean plate	(CATRF2014)
	degrees (North)	degrees (West)	mm/yr northward	mm/yr eastward	mm/yr northward	mm/yr eastward
ABD0	16.4743	61.4880	14.62 ± 0.92	10.49 ± 1.02	-0.83	-0.33
ABE1	16.4720	61.5090	16.02 ± 0.33	11.24 ± 0.32	0.58	0.42
ABMF	16.2623	61.5275	15.02 ± 0.20	10.76 ± 0.20	-0.23	-0.17
ADE0	16.2970	61.0860	16.02 ± 0.34	10.79 ± 0.36	0.39	-0.15
AVES	15.6670	63.6183	14.28 ± 1.30	10.65 ± 2.40	-0.19	-0.44
BGGY	17.0450	61.8610	15.81 ± 0.20	10.13 ± 0.20	0.53	-0.36
CAYS	15.7951	79.8461	6.30 ± 0.24	10.01 ± 0.49	-0.19	-0.20
CN01	17.0484	61.7654	15.93 ± 0.20	10.58 ± 0.24	0.61	0.09
CN04	14.0240	60.9740	15.54 ± 0.20	12.24 ± 0.20	-0.14	0.11
CN10	17.4152	75.9706	8.51 ± 0.20	8.64 ± 0.20	0.04	-0.78
CN11	17.0212	77.7841	7.89 ± 0.20	9.14 ± 0.20	0.34	-0.43
CN47	13.7108	60.9405	15.30 ± 0.20	12.50 ± 0.20	-0.40	0.21
CN48	15.4388	61.4216	14.80 ± 0.25	10.69 ± 0.29	-0.68	-0.67
CN49	15.6672	63.6183	14.11 ± 0.50	11.20 ± 0.38	-0.36	0.11
CRO1	17.7569	64.5843	13.53 ± 0.20	10.23 ± 0.20	-0.49	0.33
DESI	16.3040	61.0740	15.76 ± 0.42	10.93 ± 0.39	0.13	-0.01
DSD0	16.3120	61.0660	16.24 ± 0.70	10.15 ± 0.60	0.60	-0.78
FFT2	14.6015	61.0633	15.20 ± 1.09	12.48 ± 1.53	-0.44	0.66
FSDC	14.7350	61.1470	15.90 ± 0.49	12.07 ± 0.50	0.30	0.32
GOSI	16.2060	61.4810	15.90 ± 0.34	11.50 ± 0.34	0.45	0.54
GRE0	12.2218	61.6405	15.12 ± 0.20	13.19 ± 0.20	-0.26	0.18
LAM0	14.8130	61.1631	15.83 ± 0.32	11.56 ± 0.51	0.23	-0.15
LMMF	14.5948	60.9962	15.53 ± 0.20	12.48 ± 0.20	-0.14	0.65
MAG2	15.8900	61.3060	15.55 ± 0.33	11.82 ± 0.32	0.02	0.68
PUEC	14.0421	83.3820	5.17 ± 1.10	10.50 ± 2.00	0.54	-0.52

These estimated rotation rates correspond to a counterclockwise rotation rate (ω) of 5.585 nrad/yr about a pole that pierces Earth's surface at φ = 32.04°N and λ = 92.28°W. It is important to emphasize that these Euler-pole parameters are relative to the IGS14 reference frame.

Table 2 presents estimated Euler-pole parameters for several tectonic plates relative to ITRF2014/IGS14. This set of parameters were employed to determine the preliminary IGS14 horizontal velocities for points located on the seven tectonic plates, and then these preliminary velocities were involved in the previously described estimation process to obtain an improved horizontal velocity field for the entire region involved in this study.

Table 2. Plate rotation rates relative to ITRF2014/IGS14 as encoded into TRANS4D (version 0.3) (positive rotation rates are counterclockwise).

Plate	ω_x (nrad/yr)	ω_y (nrad/yr)	ω_z (nrad/yr)	Source
North America	0.2668	-3.3677	-0.2956	Ding et al. (2019)[#]
Caribbean	-0.88	-4.730	2.963	This paper
Pacific	-1.983	5.076	-10.516	Altamimi et al. (2017)
Cocos	-10.380	-14.901	9.133	DeMets et al. (2010)*
South America	-1.309	-1.459	-0.679	Altamimi et al. (2017)
Nazca	-1.614	-7.486	7.869	Altamimi et al. (2017)
Panama	2.088	-23.037	6.729	Kreemer et al. (2014)*
North Andes	-1.964	-1.518	0.400	Mora-Páez et al. (2019)**

[#] Ding et al. (2019) provides both rotation rates and translation rates for describing the motion of the "stable" North American plate relative to ITRF2008/IGS08 as specified in their Table2 for their ITRF-GEO-ICE6G model after outlier detection. For this study, only their rotation rates (and not their translation rates) were used to approximate the North American plate's motion relative to ITRF2014/IGS14.

* DeMets et al. (*2010)* and Kreemer et al. (2014) provide rotation rates for the Cocos and Panama plates, respectively, relative to the Pacific plate. Those rates were converted to rates relative to ITRF2014/IGS14 by using rates for the Pacific plate relative to ITRF2014/IGS14 as published by Altamimi et al. (2017).

** Mora-Páez et al. (2019) provides rotation rates for the North Andes plate relative to the South American plate. Those rates were converted to rates relative to ITRF2014/IGS14 by using the rates for the South American plate relative to ITRF2014/IGS14 as published by Altamimi et al. (2017).

Estimated Horizontal Velocities

Figure 4 presents the available stage-2 horizontal velocities relative to the fixed Caribbean plate as defined by the estimated Euler-pole parameters. Figure 5 presents a map presenting the estimated stage-3 horizontal velocities relative to this fixed Caribbean plate. Figure 6 presents the value of the larger of two standard deviations associated with stage-3 horizontal velocities, that is, the standard deviation for the velocity's north-south component and that for its east-west component.

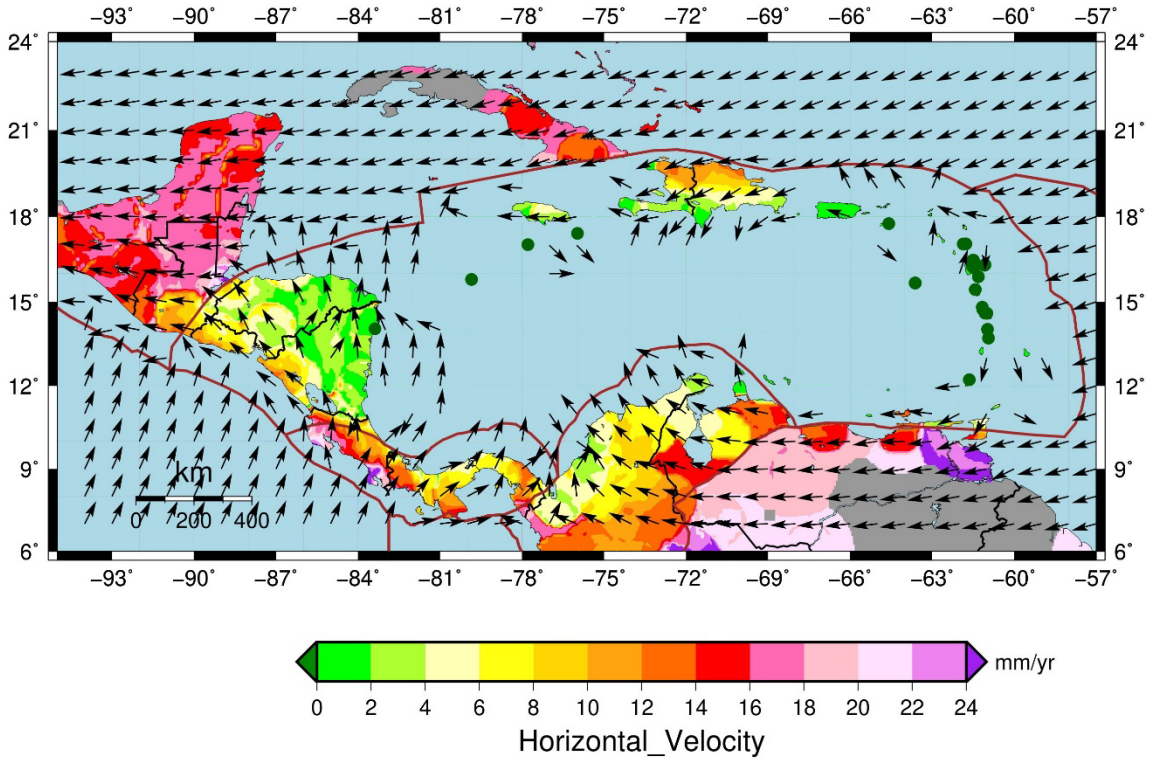

Fig. 5. Stage-3 horizontal velocities relative to a reference frame in which the "stable" part of the Caribbean plate is held fixed. Colors (other than gray and blue) indicate speed and arrows indicate direction when the corresponding speed exceeds 1.0 mm/yr. The green disks identify the 25 geodetic stations employed to estimate the Euler-pole parameters defining this reference frame. Gray areas identify large land masses where standard deviations for the stage-3 horizontal velocities exceed 2.0 mm/yr in either the east-west or north-south dimension.

Upon studying Table 1, it becomes apparent that the transformation of IGS14 horizontal velocities to horizontal velocities relative to the stable interior of the Caribbean plate can involve changes on the order of 10 mm/yr in both the north-south dimension and the east-west dimension. The magnitude of the velocity change at a point depends upon the distance between this point and the point where the Euler pole pierces Earth's surface and upon the magnitude of the rotation rate ω. Changes in vertical velocities, however, are small -- approximately 0.1 mm/yr in magnitude -- which is generally below the accuracy with which vertical velocities can currently be measured using repeated GNSS observations. Nevertheless, vertical velocities will change because Euler pole rotations pertain to representing the Earth's surface as a sphere, whereas Earth's surface is better approximated as an ellipsoid of revolution.

As presented in Figures 4, many of the 25 stations, that are involved in determining the Euler-pole parameters for the Caribbean plate, reside on a north-south trending chain of islands comprising part of the Lesser Antilles. However, near the northern extent of this island chain, a cluster of three stations are moving essentially northward at a rate of approximately 7 mm/yr. These three stations reside near the Soufriere Hills Volcano located on the island of Montserrat.

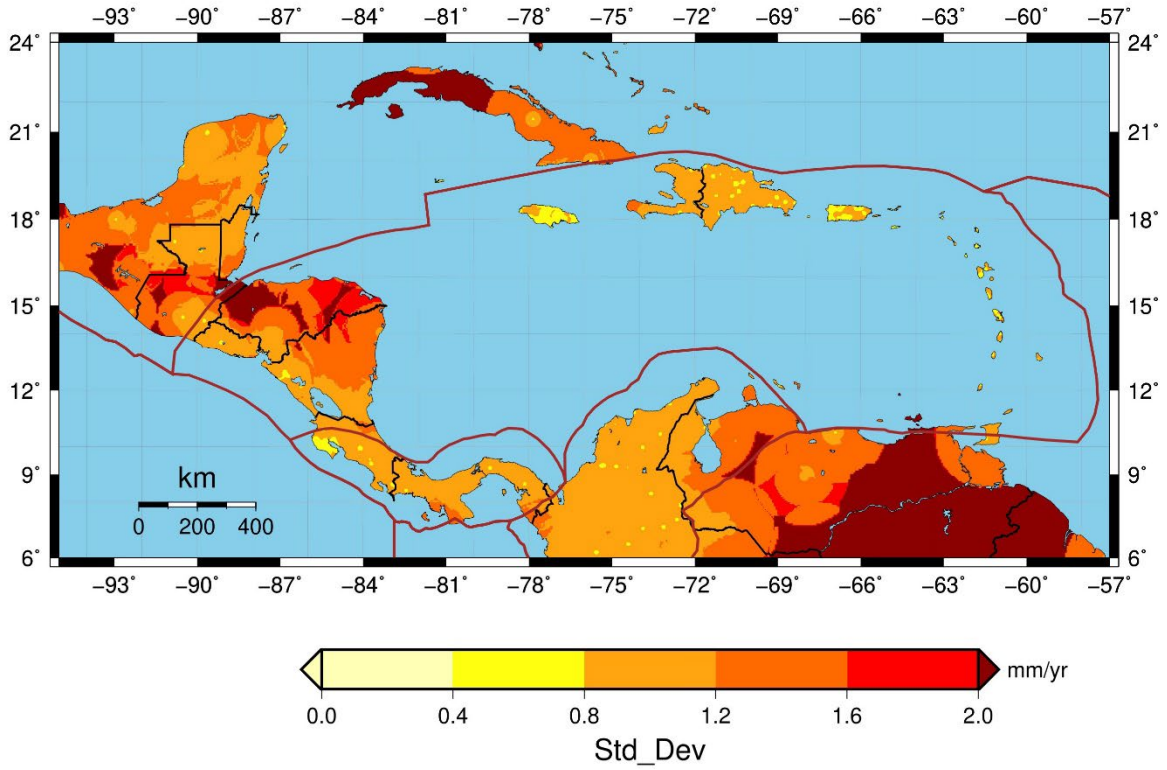

Fig 6. Map showing the larger of the standard deviation for the north-south component and the standard deviation for the east-west component of the stage-3 IGS14 horizontal velocities for locations within the large land masses of the study area.

Toward a new Caribbean reference frame

In 2024 or 2025, NGS will modernize the National Spatial Reference System (NSRS) that provides coordinates for designated locations in the United States and its territories. NGS recently published a document (NGS, 2017) that addresses the geometric aspects of the forthcoming NSRS modernization. The NSRS currently includes three geometric reference frames (historically called 'horizontal datums') which are known as NAD 83(2011), NAD 83(PA11) and NAD 83(MA11), referenced to the North America, Pacific, and Mariana tectonic plates, respectively. These reference frames are used to define the geodetic latitudes, geodetic longitudes and ellipsoid heights for points located in the USA and its territories. These three frames will be replaced with four new reference frames, to be called:

- North American Terrestrial Reference Frame of 2022 (NATRF2022)
- Pacific Terrestrial Reference Frame of 2022 (PATRF2022)
- Caribbean Terrestrial Reference Frame of 2022 (CATRF2022)
- Mariana Terrestrial Reference Frame of 2022 (MATRF2022).

According to NGS (2017): "The time-dependent Cartesian coordinates of any point on Earth in any of these four frames [*x, y, z*] will be defined as: (a) identical to (at epoch t_0) and (b) relative to (at epoch $t = t_0 + \Delta t$) the time-dependent Cartesian coordinates in the latest pre-2022 global reference frame [*X, Y, Z*] from the IGS. The relative relationship over time will rely on an NGS-determined plate motion model for the tectonic plate associated with each frame. This relationship will resemble a traditional 14 parameter transformation, but only three (time-dependent rotations about the three IGS axes) will be non-zero.

"Such time-dependent coordinates will exhibit stability in areas of the continent where motion of the tectonic plate is fully characterized by plate rotation. All remaining velocities (including horizontal motions induced directly or indirectly by adjoining tectonic plates, horizontal motions induced by Glacial Isostatic Adjustment, other horizontal motions and all vertical motion in their entirety) will be captured by an Intra-Frame Velocity Model (IFVM). Such a model will allow users to compare time-dependent coordinates in any of the four terrestrial reference frames, across years."

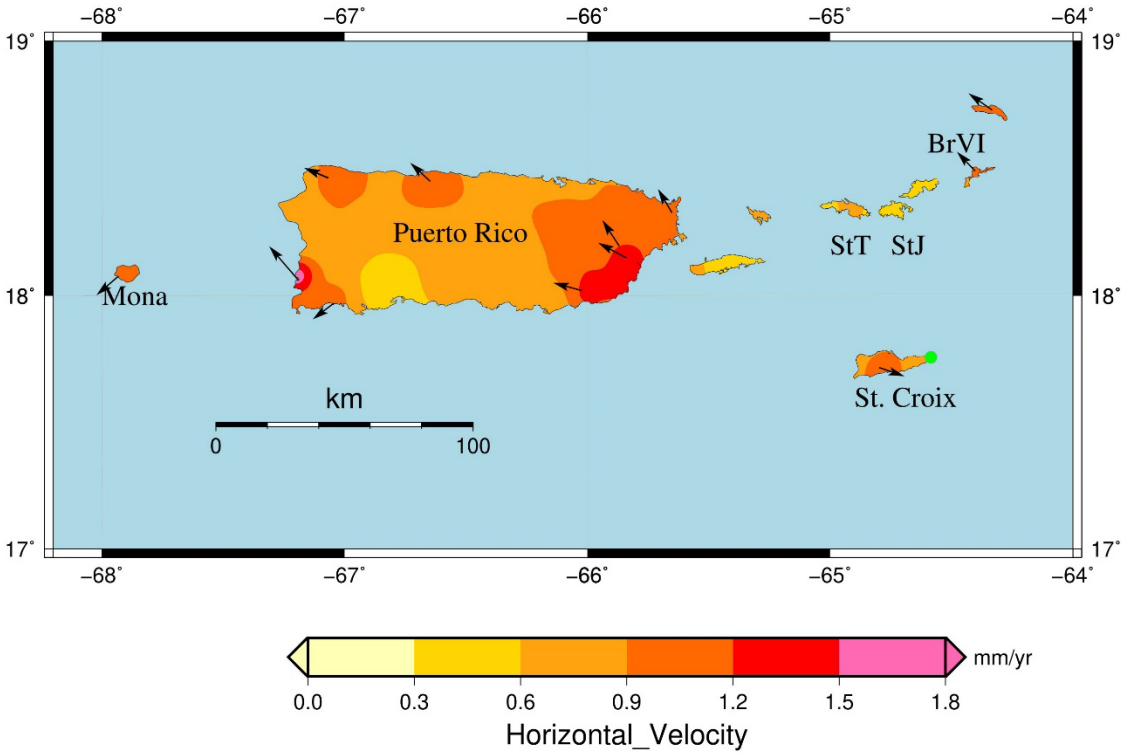

Fig. 7. Map of horizontal velocities relative to the CATRF2014 reference frame in the vicinity of Puerto Rico and the U.S. Virgin Islands. Vectors represent stage-3 horizontal velocities at those geodetic stations where such velocities have magnitudes exceeding 1.0 mm/yr. The green disk identifies a geodetic station (called CROI) involved in estimating Euler-pole parameters for the Caribbean plate. StT = Saint Thomas, StJ = St. John, and BrVI = British Virgin Islands.

NGS (2017) further states that the three "time dependent rotations" for a particular plate will equate to the three rotation rates characterizing the Euler-pole parameters for that plate. In addition, NGS (2017) acknowledges that the Euler-pole parameters for the Caribbean plate were rather uncertain at the time that the document was written. Thankfully, the availability of additional geodetic data since then provides much more reliable estimates for the Euler-pole parameters of the Caribbean plate, as documented in this paper. If NGS were to adopt the new Euler-pole parameters provided by this study, then Figure 2 illustrates estimated vertical velocities that would be associated with the IFVM for CATRF2022 and Figure 5 illustrates estimated horizontal velocities that would be associated with this IFVM. However, more accurate estimates for the Euler-pole parameters of the Caribbean plate and for its associated IFVM velocities may become available before the CATRF2022 is adopted. Thus, the velocities relative to the Euler pole parameters, given in this paper, will be identified as belonging to the CATRF2014 reference frame. Mathematical details for transforming IGS14 positional coordinates to CATRF2014 positional coordinates are presented in Appendix A of this document.

Puerto Rico and the U.S. Virgin Islands

In addition to providing a reference frame for the United States, NGS is responsible for providing official reference frames for U.S. territories. In the vicinity of the Caribbean plate, these territories include Puerto Rico and the U.S. Virgin Islands. Figure 7 presents a map of the area around these two territories and the horizontal velocity field that would result if NGS were to adopt the values of the Caribbean Euler-pole parameters estimated herein. Note that Puerto Rico includes the largest island shown in Figure 7 plus the two smaller islands located to the immediate east of this largest island. Also note that the U.S. Virgin Islands include St. Thomas, St. John, and Saint Croix as identified in Figure 7. The remaining islands located in the northeastern corner of Figure 7 are part of the British Virgin Islands, and the island to the west of Puerto Rico is called Mona.

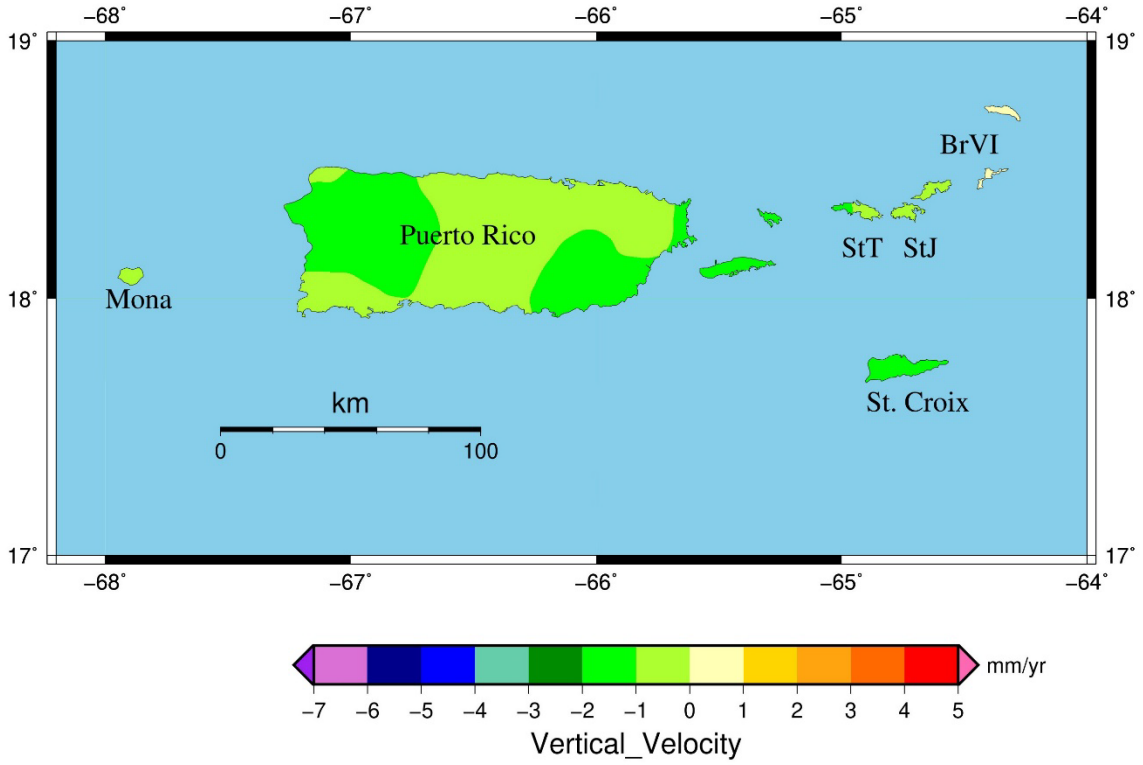

Fig. 8. Map of stage-3 IGS14 vertical velocities in the vicinity of Puerto Rico and the U.S. Virgin Islands. StT = St. Thomas, StJ = St. John, and BrVI = British Virgin Islands.

Tectonophysicists generally agree that the islands of Puerto Rico, Saint Thomas, and Saint John reside on a microplate that moves relative to the interior of the Caribbean plate (Byrne et al., 1985; Masson and Scanlon, 1991; Jansma et al., 2000; Jansma and Mattioli, 2005; Benfort et al., 2012; Liu and Wang, 2015; Symithe et al., 2015). Hence, in this study, only one geodetic station located within the area depicted in Figure 7 was employed to estimate values for this plate's Euler-pole parameters (namely, station CROI located near the extreme eastern extent of St. Croix). As a result, locations in Puerto Rico move essentially westward at a speed between 0.3 and 1.8 mm/yr, and locations in the U.S. Virgin Islands move horizontally at speeds between 0.3 and 1.2 mm/yr relative to CATRF2014. Furthermore, Figure 8 presents a map of stage-3 IGS14 vertical velocities for the same area. These velocities correspond to subsidence rates ranging between -2.0 and 0.0 mm/yr. It is also expected that any newer IGS reference frame adopted within the next few years should provide velocities that differ only insignificantly from the current IGS14 velocities (except in such cases as the occurrence of a nearby earthquake).

Summary

This document introduces version 0.3 of the TRANS4D software. This version provides a 3-D velocity model for a neighborhood of the Caribbean plate in the form of a 2-D grid (in latitude and longitude) which has a mesh of 0.0625° × 0.0625°. While the 3-D velocities, that are stored in TRANS4D, are referred to the IGS14 reference frame, this software is capable of transforming them to several other popular reference frames, plus to the newly introduced reference frame, called CATRF2014. The transformation from IGS14 to this latter reference frame is defined in terms of three Euler-pole parameters that quantify the horizontal motion of the "stable" interior of the Caribbean plate relative to the IGS14 reference frame. As such, the 25 geodetic stations that are thought to reside in this plate's "stable" interior each has a horizontal velocity with a magnitude smaller than 1.0 mm/yr relative to CATRF2014.

Appendix A: Transforming Positional Coordinates

Within the context of TRANS4D, positional coordinates for a location are assumed to vary with respect to time. Thus, when specifying positional coordinates, it is necessary to also specify the time to which they refer. Let $X(t)_a$, $Y(t)_a$, and $Z(t)_a$ denote the positional coordinates of a location at time t referred to reference frame a in a 3-D Earth-centered-Earth-Fixed (ECEF) Cartesian coordinate system. Similarly, let $X(t)_b$, $Y(t)_b$, and $Z(t)_b$ denote the positional coordinates of this same location at time t referred to reference frame b also in a 3-D-ECEF Cartesian coordinate system. Within TRANS4D, the coordinates in frame a are approximately related to those in frame b (both at time t) via the following equations of a 14-parameter transformation:

$$X(t)_b = T_x(t) + [1 + S(t)]X(t)_a + R_z(t)Y(t)_a - R_y(t)Z(t)_a$$

$$Y(t)_b = T_y(t) - R_z(t)X(t)_a + [1 + S(t)]Y(t)_a + R_x(t)Z(t)_a$$

$$Z(t)_b = T_z(t) + R_y(t)X(t)_a - R_x(t)Y(t)_a + [1 + S(t)]Z(t)_a \quad . \qquad (A1)$$

Here x, y, and z represent rectilinear coordinates expressed in meters, and t represents time expressed in years. Furthermore, $T_x(t)$, $T_y(t)$ and $T_z(t)$ are translations along the x-, y- and z-axis, respectively, each expressed in meters; and $R_x(t)$, $R_y(t)$ and $R_z(t)$ are counterclockwise rotations about these same three axes, each expressed in radians; and $S(t)$ is a unitless quantity representing the differential scale between reference frame a and reference frame b. These approximate equations suffice because the three rotations have relatively small magnitudes. Note that each of the seven quantities is represented as a function of time because modern geodetic technology has enabled scientists to detect their time-related variations with some degree of accuracy. In TRANS4D, these time-related variations are assumed to be linear, so that

$$T_x(t) = T_x(t_0) + \dot{T}_x \cdot (t - t_0) \qquad (A2)$$

$$T_y(t) = T_y(t_0) + \dot{T}_y \cdot (t - t_0)$$

$$T_z(t) = T_z(t_0) + \dot{T}_z \cdot (t - t_0)$$

$$S(t) = S(t_0) + \dot{S} \cdot (t - t_0)$$

$$R_x(t) = R_x(t_0) + \dot{R}_x \cdot (t - t_0)$$

$$R_y(t) = R_y(t_0) + \dot{R}_y \cdot (t - t_0)$$

$$R_z(t) = R_z(t_0) + \dot{R}_z \cdot (t - t_0)$$

where t_0 denotes a prespecified time of reference (expressed in years). Also, the seven quantities of the form $P(t_0)$ plus the seven quantities of the form $\dot{P}$ are constants. Note that a dot over a variable represents the rate of the corresponding variable with respect to time (in years). Thus, the seven equations of *A2* give rise to 14 parameters, but note that the values of seven of these parameters depend on the value chosen for t_0.

In the special case of a transformation from IGS14 coordinates to CATRF2014 coordinates,

$$\dot{T}_x = \dot{T}_y = \dot{T}_z = \dot{S} = 0 \qquad \text{and}$$

$$(\dot{R}_x\ ,\ \dot{R}_y\ ,\ \dot{R}_z) = (\omega_x\ ,\ \omega_y\ ,\ \omega_z) = (-0.188\ ,\ -4.730\ ,\ 2.963)\ \text{nrad/yr}\ . \qquad \text{(A3)}$$

Furthermore, if t_0 is set equal to 2010.00 which is the adopted reference epoch of the currently published IGS14 coordinates, then

$$T_x(t_0) = T_y(t_0) = T_z(t_0) = S(t_0) = R_x(t_0) = R_y(t_0) = R_z(t_0) = 0 \qquad \text{(A4)}$$

and Equation *A1* becomes

$$x(t)_b = x(t)_a + [\omega_z \cdot y(t)_a - \omega_y \cdot z(t)_a] \cdot (t - 2010.00)$$

$$y(t)_b = y(t)_a + [\omega_x \cdot z(t)_a - \omega_z \cdot x(t)_a] \cdot (t - 2010.00)$$

$$z(t)_b = z(t)_a + [\omega_y \cdot x(t)_a - \omega_x \cdot y(t)_a] \cdot (t - 2010.00) \qquad \text{(A5)}$$

where the subscript *a* identifies IGS14 coordinates and the subscript *b* identifies CATRF2014 coordinates, both referred to an arbitrary time, denoted as *t*.

From Equation *A5*, it follows that to compute a location's coordinates at time *t* relative to the CATRF2014 reference frame, then the IGS14 coordinates for this location at time *t* needs to be determinable. This may be done by knowing the location's IGS14 positional coordinates at some arbitrary time together with knowing this location's IGS14 velocity.

Also, from Equation *A5,* it follows that the CATRF2014 positional coordinates for a location equal the location's IGS14 positional coordinates when $t = 2010.00$.

Data Availability: The TRANS4D (version 0.3) software is written in FORTRAN-90. This software, together with its associated data files and User's Guide, may be obtained by contacting Richard Snay (Email: rssnay@aol.com).

Acknowledgments

The authors thank the many people and institutions that were involved in collecting and/or processing the geodetic data included in this study. The authors also thank Daniel Gillins and an anonymous reviewer for suggestions that improved the presentation of this paper. This paper was supported, in part, by the National Geodetic Survey. The figures have been drawn using *Generic Mapping Tools* (Wessel and Smith, 1998).

References:

Altamimi, Z., X. Collilieux, and L. Metivier. 2011. "ITRF2008: an improved solution of the International Terrestrial Reference Frame." *Journal of Geodesy, 85(8)*. https://doi.org/10.1007/s00190-011-0444-4

Altamimi, Z., P. Rebischung, L. Metivier, and X. Collilieux, 2016. "ITRF2014: A new release of the International Terrestrial Reference Frame modelling non-linear station motions." *Journal of Geophysical Research: Solid Earth, 121*. https://doi.org/10.1002/2016JB013098

Altamimi, Z., L. Metivier, P. Rebischung, H. Rouby, and X. Collilieux. 2017. "ITRF2014 plate motion model. *Geophysical Journal International",* 209. https://doi.org/10.1093/gji/ggx136

Benford, B., C. DeMets, B. Tikoff, P. Williams, L. Brown, M. Wiggins-Grandison. 2012. "Seismic hazard along the southern boundary of the Gônave microplate: block modeling of GPS velocities from Jamaica and nearby islands, northern Caribbean." *Geophysical Journal International, 190(1),* 59-74.

Bird, P. 2003. "An updated digital model of plate boundaries." *Geochem. Geophys. Geosyst., 4(3),* 1027. https://doi.org/10.1029/2001GC000252 .

Blewitt, G., W. C. Hammond, and C. Kreemer. 2018. "Harnessing the GPS data explosion for interdisciplinary science." *Eos*, 99. https://doi.org/10.1029/2018EO104623 .

Bock, Y., and F. Webb. 2012. "MEaSUREs Solid Earth Science ESDR System." La Jolla, California and Pasadena, California, USA. http://sopac-ftp.ucsd.edu/pub/timeseries/measures/timeseriesModelTermsSummary.MEASURES_Combination.20130627.txt .

Byrne, D. B., G. Suarez, and W. R. McCann. 1985. "Muortos trough subduction-microplate tectonics in the northern Caribbean?" *Nature, vol.317(6036),* 420-421.

DeMets, C., R. G. Gordon, and D. F. Argus. 2010. "Geologically current plate motions." *Geophys. J. Int., 181.* https://doi.org/10.1111/j.1365-246X.2009.04491.x .

Ding, K., J. T. Freymueller, P. He, Q. Wang, and C. Xu. 2019.] "Glacial isostatic adjustment, intraplate strain, and relative sea level changes in eastern United States." *J. Geophysical Research, 124*. https://doi.org/10.1029/2018JB017060 .

Ellis, A., C. DeMets, P. Briole, B. Cosenza, O. Flores, S. Graham, et al. 2018. "GPS constrains on deformation in northern Centra America from 1999 to 2017, Part 1: Time-dependent modelling of large regional earthquakes and their post-seismic effects." *Geophys. J. Int.,* 215. https://doi.org/10.1093/gji/ggy249

Ellis, A., C. DeMets, R. McCaffrey, P., Briole, B., Cosenza Muralles, et al. 2019. "GPS constraints on deformation in northern Central America from 1999 to 2017, Part 2: Block rotations and fault slip rates, fault locking and distributed deformation." *Geophys. J. Int., 218*. https://doi.org/10.1093/gji/ggz173 .

Goovaerts, P. 1997. *Geostatistics for Natural Resources Evaluation*, Oxford University Press, ISBN 0-19-511538-4.

Herring, T. A., T. I. Melbourne, M. H. Murray, M. A. Floyd, W. M. Szeliga, R. W. King, R. W., …, L. Wang. 2016. "Plate Boundary Observatory and related networks: GPS data analysis methods and geodetic products." *Reviews of Geophysics, 54*. https://doi.org/10.1002/2016RG000529 .

Jansma, P. E., G. S. Mattioli, A. Lopez, et al. 2000. "Neotectonics of Puerto Rico and the Virgin Islands, northeastern Caribbean, from GPS geodesy." *Tectonics, 19(6),* 1021-1037.

Jansma, P. E. and G. S. Mattioli. 2005. "GPS results from Puerto Rico and the Virgin Islands: constraints on tectonic setting and rates of active faulting." *GSA Special Papers, 85*, 13-30.

Kreemer, C., G. Blewitt, and E. C. Klein. 2014. "A geodetic plate motion and global strain rate model." *Geochem. Geophys. Geosyst., 15*. https://doi.org/10.1002/2014GC005407 .

Liu, H. and G. Wang. 2015. "Relative motion between St. Croix and the Puerto Rico-Northern Virgin Islands block derived from continuous GPS observations (1995 – 2014)." *International Journal of Geophysics, 2015*. https://doi.org/10.1155/2015/915753

Masson, D. G. and K. M. Scanlon. 1991. The neotectonics setting of Puerto Rico. *Geological Society of America Bulletin, 103(1)*, 144-154, 1991.

McCaffrey, R., R. W. King, S. J. Payne, and M. Lancaster. 2013. "Active tectonics of northwestern U.S. inferred from GPS-derived surface velocities." *Journal of Geophysical Research: Solid Earth, 118*. https://doi.org/10.1029/2012JB009473

Mora-Páez, H., J. N. Kellogg, J. T. Freymueller, D. Mencin, D., R. M. S. Fernandes, H., Diederix, H., … Y. Corchuelo-Cuevo. 2019. Crustal deformation in the northern Andes – A new GPS velocity field." *Journal of South American Earth Sciences, 89,* pp. 76-91. https://doi.org/10.1016/j.jsames.2018.11.002

Moritz, H. 2000. "Geodetic Reference System 1980." *Journal of Geodesy, 74(1),* pp. 128-162. https://doi.org/10.1007/s001900050278 , ftp://athena.fsv.cvut.cz/ZFG/grs80-Moritz.pdf

NGS. 2017, "Blueprint for 2022, Part 1: Geometric Coordinates." *NOAA Technical Report NOS NGS 62, 32 pp.* https://geodesy.noaa.gov/library/pdfs/NOAA_TR_NOS_NGS_0062.pdf

NGS. 2020. "Delayed release of the modernized NSRS." *NSRS Modernization News*, Issue 20, June 2020. https://geodesy.noaa.gov/datums/newdatums/NSRSModernizationNewsIssue20.pdf

Rebischung, P., Z. Altamimi,J. Ray, and B. Garayt. 2016. "The IGS contribution to ITRF2014." *Journal of Geodesy.* https://doi.org/10.1007/s00190-016-0897-6

Rebischung, P. and R. Schmidt. 2016. “IGS/igs.atx: a new framework for the IGS products.” 2016 AGU Fall Meeting, San Francisco.

Rebischung, P., J. Griffiths, J. Ray, R., Schmid, X. Collilieux, and B. Garayt. 2012. “IGS08: The IGS realization of ITRF2008”, *GPS Solutions, 16*. https://doi.org/10.1007/s10291-011-0242-2

Saleh, J., S. Yoon, K. Choi, L. Sun, R. Snay, P. McFarland, S. Williams, D. Haw, F. Coloma. 2021. “1996—2017 GPS position time series, velocities and quality measures for the CORS network.” Journal of Applied Geodesy. https://doi.org/10.1515/jag-2020-0041

Sánchez, L. and H. Drewes. 2020 “Geodetic monitoring of variable surface deformation in Latin America. International Association of Geodesy Symposia Series.” Vol. 152. https://doi.org/10.1007/1345_2020_91

Shen, Z.-K., R, King, D. C. Agnew, M. Wang, T. A. Herring, D. Dong, and F. Fang. 2011. “A unified analysis of crustal motion in southern California, 1970—2004: The SCEC crustal motion map.” *Journal of Geophysical Research, 116,* B11402. https://doi.org/10.1029/2011JB008549

Snay, R. A., J. T. Freymueller, M. R. Craymer, C. F. Pearson, and J. Saleh. 2016. “Modeling 3-D crustal velocities in the United States and Canada.” *Journal of Geophysical Research: Solid Earth*, *121*. https://doi.org/10.1002/2016JB012884

Snay, R. A., J. Saleh, and C. F. Pearson. 2018.] “Improving TRANS4D’s model for vertical crustal velocities in western CONUS.” *Journal of Applied Geodesy*, *12(3)*. https://doi.org/10.1515/jag-2018-0010

Symithe, S., E. Calais, J. B. de Chabalier, R. Robertson, and M. Higgins. 2015.] “Current block motions and strain accumulation on active faults in the Caribbean.” *Journal of Geophysical Research: Solid Earth,* 120. https://doi.org/10.1002/2014JB011779

Wang, G., H. Liu, G. S. Mattioli, M. M. Miller, K. Feaux, and J. Braun. 2019. “A stable geodetic reference frame for geological hazard monitoring in the Caribbean region.” *Remote Sensing, 11*, 680. https://doi.org/10.3390/rs11060680

Wessel, P., and W. H. F. Smith. 1998. “New improved version of generic mapping tools released.” Eos Trans. AGU, 79(47), 579. doi:10.1029/98EO00426